Available online at www.sciencedirect.com
SCIENCE DIRECT®
International Journal of Thermal Sciences 43 (2004) 297–306
International Journal of Thermal Sciences
www.elsevier.com/locate/ijts

# Determination of the thermal resistance of walls through a dynamic analysis of in-situ data

Lucio Laurenti, Fulvio Marcotullio *, Filippo de Monte

*Dipartimento di Energetica, Università di L'Aquila, Località Monteluco 67040, Roio Poggio (AQ), Italy*

Received 26 May 2003; accepted 5 August 2003

**Abstract**

In this paper a method for calculating the thermal resistance of a wall through the dynamic analysis of both heat flux and surface temperature samples is presented. Such a method models the transient thermal response of the wall through a linear relation with constant parameters that links the instantaneous heat flux at the inner surface of the wall to the temperature difference between the surfaces of the same wall at the same instant. Additionally, the linear relation mentioned above also links a certain number $p$ of terms formed, each of them, by differences of the same variables related to the considered instant and to $p$ previous instants. The number of the parameters of the model is derived through the principles of hypothesis testing. At this stage, the proposed method is applied to simulated data as indicated by the proposal of European standard 12494, 1996. The results shown here have been concerning with different typologies of wall, namely light, medium and heavy, as well as with 24 data sets obtained by picking data in the one-year time series. Although limited to winter and summer measurement periods, a comparison between the proposed method and classic average one is also performed.


*Keywords:* Thermal resistance; Transmittance; Heat flow; Measuring; Indoor temperature; Outdoor temperature; Light wall; Medium wall; Heavy wall

## 1. Introduction

The experimental determination of the thermal resistance of walls always represents a problem of practical interest in the field of the buildings thermal analyses as well as of the energy saving. In past years the experimental activity was made solely in laboratory by using prototypes of walls in real scale realised on purpose. In particular, the used test facility, designed and built following careful directives which were object of an ample set of international standards [1–3], was able to determine the searched quantity through measurements of both surface temperatures and heat flux related to a wall in steady-state condition.

However, this experimental activity was not cost-effective because of the manufacture of the prototype and of its subsequent transport in the measurement laboratory, where large rooms, as well as suitable devices for prototype handling, were strictly necessary. Additionally, the experimental activity mentioned above was not cost-effective also because of the prototype demolition and subsequent removal of the wreckage. Also it needs to consider that, notwithstanding the extreme accuracy of the measurement in laboratory, the thermal resistance of the wall determined in situ might present a nonnegligible deviation from the one determined on a prototype. This deviation is due not only to the inevitable differences among supplies of the same material made in different periods, but also and above all to the inevitable differences in the conditions of wall-laying.

It should be noted that there exist in every respect particular cases in which the experimental determination of the thermal resistance of the wall must necessarily be made in laboratory (there is no alternative). They concern the design of prefabricated building, the certification of building components as provided in the tender, and so on. Contrarily, there exist many other cases in which the determination of the thermal resistance of walls cannot be carried out in a laboratory because the walls are exactly the walls of an actual building. In these cases it would be desirable and of great usefulness to evaluate the resistance in situ. Behaving like this, we can get not only a large reduction of the costs but also the complete elimination of the uncertainties due to the use of prototypes which (as pointed out above) are inevitably different from the element under consideration.

* Corresponding author.
*E-mail address:* marcotul@ing.univaq.it (F. Marcotullio).

1290-0729/$ – see front matter 
doi:10.1016/j.ijthermalsci.2003.08.007

**Nomenclature**

| | | | |
|---|---|---|---|
| $a(t)$ | generic thermal response at a given location within $\Omega$ (in this case, the surface heat flux $q$) | $\widehat{R}$ | estimated thermal resistance of the wall ... $m^2{\cdot}K{\cdot}W^{-1}$ |
| $\mathbf{a}(t)$ | vector of $(B+1)$ length whose transposed is defined as $\mathbf{a}^T = \{a, \tilde{\mathbf{a}}\}$ | $\overline{R}$ | final estimate of thermal resistance of the wall ... $m^2{\cdot}K{\cdot}W^{-1}$ |
| $\tilde{\mathbf{a}}(t)$ | vector containing $B$ generic thermal inputs (known) | $R_{LS}$ | sum of squares of residuals ... $W^2{\cdot}m^{-4}$ |
| $\mathbf{a}_{n+j}$ | values of the vector $\mathbf{a}$ at the nodal location $\xi = j$ | $s$ | thickness of the wall ... m |
| $b_1$ | unknown constant parameters ... $m^2{\cdot}W^{-1}$ | $T_{is}$ | inner surface temperature ... K |
| $b_2, b_3$ | unknown constant parameters ... $K^{-1}$ | $T_{os}$ | outer surface temperature ... K |
| $B$ | number of the generic thermal inputs | $T$ | period of the thermal inputs ... s |
| $c$ | specific heat ... $J{\cdot}kg^{-1}{\cdot}K^{-1}$ | $t$ | time ... s |
| $F_{1-\alpha}$ | lower limit of the critical region | *Greek symbols* | |
| $\mathbf{I}$ | identity matrix | $\alpha$ | significance level of the test |
| $k$ | thermal conductivity ... $W{\cdot}m^{-1}{\cdot}K^{-1}$ | $\beta$ | unknown constant parameters ... $m^2{\cdot}K{\cdot}W^{-1}$ |
| $\mathbf{M}_i$ | $1 \times (B+1)$ condensed matrices | $\boldsymbol{\beta}$ | vector of the $\beta$ parameters ... $m^2{\cdot}K{\cdot}W^{-1}$ |
| $M$ | number of $\boldsymbol{\beta}$ components | $\hat{\boldsymbol{\beta}}$ | vector of estimated $\beta$ parameters ... $m^2{\cdot}K{\cdot}W^{-1}$ |
| $N_{n+j}$ | shape function associated at the location $\xi = j$ (dimensionless) | $\Delta I$ | value of the ratio $I_{0.99}(R)/\widehat{R} \times 100$ |
| $p$ | number of $\omega$ nodal points (Fig. 1) | $\Delta t$ | sampling interval ... s |
| $q$ | surface heat flux ... $W{\cdot}m^{-2}$ | $\nu$ | number of the degrees of freedom |
| $\mathbf{q}$ | vector containing the samples of surface heat flux ... $W{\cdot}m^{-2}$ | $\xi$ | dimensionless time, $= t/\Delta t$ |
| $\hat{\mathbf{q}}$ | vector containing the estimated samples of surface heat flux ... $W{\cdot}m^{-2}$ | $\rho$ | density ... $kg{\cdot}m^{-3}$ |
| $R$ | thermal resistance of the wall ... $m^2{\cdot}K{\cdot}W^{-1}$ | $\omega$ | finite element of time ... s |
| | | $\Omega$ | 3-D domain (i.e., body where the transient heat conduction takes place) |

Unfortunately, the practical realisation of the measurement in situ presents many difficulties due both to the problems connected to the accurate measurements of the surface temperatures and heat flux (number and type of sensors, their location and shielding, and so on) and above all to the practically complete impossibility to control the thermal transient. It, in fact, depends on the seasonal climatic conditions that can also happen in an unfavourable manner. All that complicates the data analysis which is basic for the identification of the wall characteristics, as an example the thermal resistance. As is well known [4], the choice of the thermal model is of primary importance to reach the aim (i.e., the thermal resistance) in the simplest way and (if it may be done) also in the rapidest way to avoiding so a redundant stop of facilities as well as useless inconveniences in case the measurements will be concerning with inhabited buildings.

The features of the test facilities regarding the measurements of the surface temperatures and heat flux, as well as the techniques for the analysis of the experimental data in order to identify the searched thermal resistance, are object of ISO standard 9869 [5].

Notwithstanding this, the model suggested in [5] and described in [6] (i.e., a linear combination of unknown parameters whose values may be derived through classical techniques of numerical regression) is not easy to use. The complexity mainly derives from (1) the lack of physical meaning for the parameters of the regression with the only exception for the sought thermal resistance, and (2) the necessity to simultaneously determine some (generally up to three) unknown time constants in an iterative procedure.

A proposal of the European standard [7] took into account largely the ISO 9869, with the only exception of the complex algorithm mentioned above. This proposal, in fact, allows various techniques for data analysis to be used provided they be classified into classes defined by the same European standard.

In this paper a new mathematical model is proposed. It allows the thermal resistance to be easily recognised and provides the discrete dynamic response of a linear system (in every respect any complex wall may be considered like that) following an original procedure described first in [8], generalised recently in [9] and used several times for accurate thermal analyses in multi-dimensional bodies [9,10]. It is interesting to point out that the obtained result, although shows some part-expected similarities with the ISO 9869, is able to identify the wall without performing further calculations and manipulations. Additionally, a statistic analysis of the parameters provides useful information to optimise the model dimension. The model dimension depends not only on the considered wall, but also on the insights contained in the measured data. It is also shown that the identification of the characteristics of the wall becomes much more difficult

when the input/output signals measured during the summer season are used instead of the ones measured during the winter season. Notwithstanding the suggested algorithm always reaches its objective, the more the system is able to amplify the lag between input and output, the more the complexity of the algorithm (which is given by the number of terms appearing in the correlation, namely, by the store extension of the remote format of the signal) increases in a significant manner.

## 2. Deriving a parametric model for the transient heat conduction

If the heat flux or temperature histories at the outer surface of a 3-D domain $\Omega$ are known as functions of time (i.e., we have $B$ thermal inputs $\tilde{\mathbf{a}}(t)$), then the thermal response $a(t)$ (temperature or heat flux) at a given location (interior or exterior) of $\Omega$ may be derived in a fairly simple manner as a solution to the following differential equation of $p-1$ order [8]:

$$\mathbf{M}_0\mathbf{a} + \sum_{i=1}^{p-1} \mathbf{M}_i \frac{\partial^i \mathbf{a}}{\partial t^i} = 0 \tag{1}$$

(where $p \geqslant 2$) provided the unsteady heat conduction problem of interest be linear. The vector $\mathbf{a}^{\mathrm{T}} = \{a, \tilde{\mathbf{a}}\}$ contains the time-dependent unknown function $a(t)$ as well as the given $B$ thermal inputs $\tilde{\mathbf{a}}(t)$. The $p$ matrices $\mathbf{M}$ of $1 \times (B+1)$ order appearing on the LHS of Eq. (1) contain terms which depend solely on the geometric characteristics and thermal properties of the domain $\Omega$.

With reference to the application which is herein of great concern (as has already been said in Section 1), the surface heat flux or temperature histories of the body which appear in the vector $\tilde{\mathbf{a}}(t)$ are determined by an experimental way. Therefore, they are given as a ordained sequence of samples corresponding to consecutive time instants, whose spacing $\Delta t$ (i.e., sampling interval) is held constant along the time-axis. In these cases it might be useful to search for a solution to Eq. (1) in a discrete form through a step-by-step procedure as shown in [11].

To this purpose, a finite domain of time $\omega$ of $(p-1)\Delta t$ length may suitably be chosen (see Fig. 1). Then, by using the symbol $\mathbf{a}_{n+j}$ $(2-p \leqslant j \leqslant 1)$ for the values assumed by the vector $\mathbf{a}$ at the nodal locations $\xi = j$ (where $\xi = t/\Delta t$), we can write

$$\mathbf{a} \approx \sum_{j=1}^{2-p} N_{n+j}\mathbf{a}_{n+j} \tag{2}$$

where only the $p$ shape functions $N_{n+j}$ depend on the local variable $\xi$. In particular, these functions represent a solution of first attempt for $a(t)$ on $\omega$ and, for this reason, they may

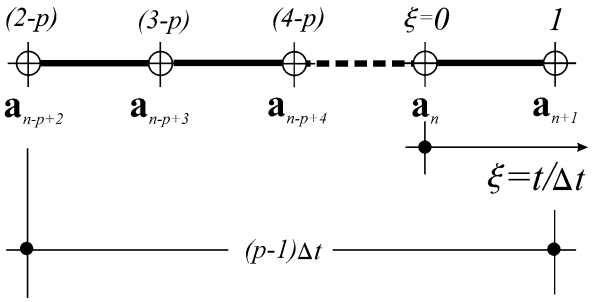


Fig. 1. Scheme of the finite domain of time.

be chosen arbitrarily provided be derivable at least up to the $p-1$ order. In such a way, the following relations are valid:

$$\frac{\partial^i \mathbf{a}}{\partial t^i} \approx \frac{1}{\Delta t^i} \sum_{j=1}^{2-p} \frac{\partial^i N_{n+j}}{\partial \xi^i}\mathbf{a}_{n+j}, \quad i = 1, 2, \ldots, p-1 \tag{3}$$

Substituting Eqs. (2) and (3) in Eq. (1), we obtain

$$\mathbf{M}_0 \sum_{j=1}^{2-p} (N_{n+j}\mathbf{a}_{n+j}) + \sum_{i=1}^{p-1} \left[ \frac{\mathbf{M}_i}{\Delta t^i} \left( \sum_{j=1}^{2-p} \frac{\partial^i N_{n+j}}{\partial \xi^i}\mathbf{a}_{n+j} \right) \right] = 0 \tag{4}$$

It is well known [11,12] that there exists a physical constraint among the $p$ shape functions, namely,

$$\sum_{j=1}^{2-p} N_{n+j} = 1$$

from which it follows:

$$N_{n+1} = 1 - \sum_{j=0}^{2-p} N_{n+j} \tag{5}$$

Furthermore, differentiating both sides of the previous equation with respect to $\xi$, we get

$$\frac{\partial^i N_{n+1}}{\partial \xi^i} = -\sum_{j=0}^{2-p} \frac{\partial^i N_{n+j}}{\partial \xi^i}, \quad i = 1, 2, \ldots, p-1 \tag{6}$$

Then, the first term on the left-hand side of Eq. (4) may be rewritten as

$$\mathbf{M}_0 \sum_{j=1}^{2-p} (N_{n+j}\mathbf{a}_{n+j}) = \mathbf{M}_0 N_{n+1}\mathbf{a}_{n+1} + \mathbf{M}_0 \sum_{j=0}^{2-p} (N_{n+j}\mathbf{a}_{n+j})$$

and, in view of Eq. (5), after some matrix steps we obtain

$$\mathbf{M}_0 \sum_{j=1}^{2-p} (N_{n+j}\mathbf{a}_{n+j}) = \mathbf{M}_0\mathbf{a}_{n+1} + \mathbf{M}_0 \sum_{j=0}^{2-p} N_{n+j}(\mathbf{a}_{n+j} - \mathbf{a}_{n+1})$$

Similarly, the second term on the left-hand side of Eq. (4) may be rewritten as

$$\sum_{i=1}^{p-1}\left[\frac{\mathbf{M}_i}{\Delta t^i}\left(\sum_{j=1}^{2-p}\frac{\partial^i N_{n+j}}{\partial\xi^i}\mathbf{a}_{n+j}\right)\right] = \sum_{i=1}^{p-1}\left[\frac{\mathbf{M}_i}{\Delta t^i}\left(\frac{\partial^i N_{n+1}}{\partial\xi^i}\mathbf{a}_{n+1}\right)+\frac{\mathbf{M}_i}{\Delta t^i}\left(\sum_{j=0}^{2-p}\frac{\partial^i N_{n+j}}{\partial\xi^i}\mathbf{a}_{n+j}\right)\right]$$

and, in view of Eq. (6), after some suitable manipulations we have

$$\sum_{i=1}^{p-1}\left[\frac{\mathbf{M}_i}{\Delta t^i}\left(\sum_{j=1}^{2-p}\frac{\partial^i N_{n+j}}{\partial\xi^i}\mathbf{a}_{n+j}\right)\right] = \sum_{i=1}^{p-1}\left\{\frac{\mathbf{M}_i}{\Delta t^i}\left[\sum_{j=0}^{2-p}\frac{\partial^i N_{n+j}}{\partial\xi^i}(\mathbf{a}_{n+j}-\mathbf{a}_{n+1})\right]\right\}$$

Finally, Eq. (4) may be taken as follows:

$$\mathbf{M}_0\mathbf{a}_{n+1}+\mathbf{M}_0\sum_{j=0}^{2-p}N_{n+j}(\mathbf{a}_{n+j}-\mathbf{a}_{n+1}) + \sum_{i=1}^{p-1}\left\{\frac{\mathbf{M}_i}{\Delta t^i}\left[\sum_{j=0}^{2-p}\frac{\partial^i N_{n+j}}{\partial\xi^i}(\mathbf{a}_{n+j}-\mathbf{a}_{n+1})\right]\right\}=0 \qquad (7)$$

The minimisation of the deviation between the exact and approximate solutions (where the approximate solution is represented by Eq. (2)) can be obtained applying the method of weighted residuals to Eq. (7) [11] and assuming that the whole domain of solution coincides with the element of time $\omega$ shown in Fig. 1. Behaving like this, we can derive the following algebraic equation able to link the samples $\mathbf{a}_{n+j}$ of $\mathbf{a}$ in $\omega$:

$$\int_\omega W(\mathbf{M}_0\mathbf{a}_{n+1})\,\mathrm{d}\xi+\int_\omega W\left(\mathbf{M}_0\sum_{j=0}^{2-p}N_{n+j}(\mathbf{a}_{n+j}-\mathbf{a}_{n+1})\right)\mathrm{d}\xi + \int_\omega W\sum_{i=1}^{p-1}\left\{\frac{\mathbf{M}_i}{\Delta t^i}\left[\sum_{j=0}^{2-p}\frac{\partial^i N_{n+j}}{\partial\xi^i}(\mathbf{a}_{n+j}-\mathbf{a}_{n+1})\right]\right\}\mathrm{d}\xi=0 \qquad (8)$$

where $W$ represents a weighting function dependent on $\xi$ whose choice is completely arbitrary and above all not basic to our purposes. As the matrices $\mathbf{M}$ and the vectors $\mathbf{a}_{n+j}$ are independent of $\xi$, Eq. (8) simplifies to

$$\mathbf{M}_0\mathbf{a}_{n+1}+\mathbf{M}_0\sum_{j=0}^{2-p}\left[\Theta_{0,j}(\mathbf{a}_{n+j}-\mathbf{a}_{n+1})\right] + \sum_{i=1}^{p-1}\frac{\mathbf{M}_i}{\Delta t^i}\sum_{j=0}^{2-p}\left[\Theta_{i,j}(\mathbf{a}_{n+j}-\mathbf{a}_{n+1})\right]=0 \qquad (9)$$

where

$$\Theta_{0,j}=\frac{\int_\omega W N_{n+j}\,\mathrm{d}\xi}{\int_\omega W\,\mathrm{d}\xi} \quad \text{and}$$

$$\Theta_{i,j}=\frac{\int_\omega W(\partial^i N_{n+j}/\partial\xi^i)\,\mathrm{d}\xi}{\int_\omega W\,\mathrm{d}\xi}$$

Additionally, setting

$$\mathbf{B}_j=\mathbf{M}_0\Theta_{0,j}+\sum_{i=1}^{p-1}\frac{\mathbf{M}_i}{\Delta t^i}\Theta_{i,j}$$

Eq. (9) may be rewritten in a more concise form as follows:

$$\mathbf{M}_0\mathbf{a}_{n+1}+\sum_{j=0}^{2-p}\mathbf{B}_j(\mathbf{a}_{n+j}-\mathbf{a}_{n+1})=0$$

Once the $p$ matrices $\mathbf{M}$ have been calculated, the values of the parameters $\Theta$ defined above may suitably be determined as indicated in Ref. [9]. Therefore, performing the matrix products which appear in Eq. (9), we finally get

$$\sum_{i=1}^{B+1}\left[b_{i,n+1}a_{i,n+1}+\sum_{j=0}^{2-p}b_{i,n+j}(a_{i,n+j}-a_{i,n+1})\right]=0 \qquad (10)$$

where $b_{i,n+1}=M_0(i)$ and $b_{i,n+j}=B_j(i)$. Eq. (10) is of great concern. It states that the samples of the dependent variable $a$ are linked to the corresponding samples of the $B$ independent variables $\tilde{\mathbf{a}}$ in correspondence of the nodal points of the time element of Fig. 1, i.e., at the instants $t=\xi\Delta t$.

Therefore, if the parameters $b$ and the initial temperature distribution within the 3-D domain $\Omega$ are given, then the relation (10) may be used in a recursive form to get the sample of the thermal response $a_{1,n+1}$ at a given instant $(n+1)\Delta t$ due to the samples of $B$ independent functions (namely, the boundary conditions of the unsteady heat conduction problem under consideration).

If, instead, the thermal properties of the solid are unknown (this case is here of interest), then the parameters $b$ of Eq. (10) may be determined provided the value of $p$ is known and an adequate number of experimental data is available.

## 3. Applying the parametric model to a conductive slab-shaped domain

Let us consider a large plate with temperature-independent material properties subject to time-dependent boundary conditions of the 1st kind at both the inner and outer surfaces of the wall. Therefore, in every respect the system under consideration may be considered one-dimensional and linear from a thermal standpoint. During the transient, the samples of the surface temperatures $T_{\mathrm{is}}$ (inner) and $T_{\mathrm{os}}$ (outer), which represent the independent variables of the problem appearing in $\tilde{\mathbf{a}}$, are measured. Similarly, the samples of the heat flux per unit of area at the inner surface of the planar layer (this quantity represents the dependent variable $a$ of

the problem) are measured. From what was previously said, it follows that $\mathbf{a}^{\mathrm{T}} = \{q, T_{\mathrm{is}}, T_{\mathrm{os}}\}$ and so Eq. (10) becomes

$$b_{1,n+1}q_{n+1} + b_{2,n+1}T_{\mathrm{is},n+1} + b_{3,n+1}T_{\mathrm{os},n+1} + \sum_{j=0}^{2-p} b_{1,j}(q_{n+j} - q_{n+1}) + \sum_{j=0}^{2-p} b_{2,j}(T_{\mathrm{is},n+j} - T_{\mathrm{is},n+1}) + \sum_{j=0}^{2-p} b_{3,j}(T_{\mathrm{os},n+j} - T_{\mathrm{os},n+1}) = 0 \tag{11}$$

Dividing both sides of the previous equation by $b_{1,n+1}$, Eq. (11) may be rewritten in such a way as to explicit the specific heat flux of interest at a given instant ($\xi = n+1$). Therefore, we obtain

$$q_{n+1} = \beta_{2,n+1}T_{\mathrm{is},n+1} + \beta_{3,n+1}T_{\mathrm{os},n+1} + \sum_{j=0}^{2-p} \beta_{1,j}(q_{n+j} - q_{n+1}) + \sum_{j=0}^{2-p} \beta_{2,j}(T_{\mathrm{is},n+j} - T_{\mathrm{is},n+1}) + \sum_{j=0}^{2-p} \beta_{3,j}(T_{\mathrm{os},n+j} - T_{\mathrm{os},n+1}) \tag{12}$$

where the generic parameter $\beta_{i,j}$ is taken as

$$\beta_{i,j} = -\frac{b_{i,j}}{b_{1,n+1}}$$

It may be noted that $\beta_{2,n+1}$ and $\beta_{3,n+1}$ are not independent between them. In fact, when the thermal equilibrium (characterised clearly by $q = 0$ and $T_{\mathrm{os}} = T_{\mathrm{is}} = \mathrm{cost} = \widetilde{T}$) is reached, Eq. (12) reduces to

$$0 = (\beta_{2,n+1} + \beta_{3,n+1})\widetilde{T}$$

from which it follows that $\beta_{3,n+1} = -\beta_{2,n+1}$. Additionally, when the steady-state temperature field is reached, Eq. (12) simplifies to

$$q = \beta_{3,n+1}(T_{\mathrm{os}} - T_{\mathrm{is}}),$$

where $\beta_{3,n+1}$ is exactly the inverse of the thermal resistance $R$ for conduction through the wall, namely, $\beta_{3,n+1} = 1/R$. On the basis of these considerations, Eq. (12) may be rewritten in the following form:

$$q_{n+1} = \frac{1}{R}(T_{\mathrm{os},n+1} - T_{\mathrm{is},n+1}) + \sum_{j=0}^{2-p} \beta_{1,j}(q_{n+j} - q_{n+1}) + \sum_{j=0}^{2-p} \beta_{2,j}(T_{\mathrm{is},n+j} - T_{\mathrm{is},n+1}) + \sum_{j=0}^{2-p} \beta_{3,j}(T_{\mathrm{os},n+j} - T_{\mathrm{os},n+1})$$

In matrix format, we have

$$q_{p,n+1} = \mathbf{X}_p^{\mathrm{T}}\boldsymbol{\beta}_p \tag{13}$$

This format allows us to emphasise that all the quantities appearing in Eq. (13) refer to the $\mathcal{M}_p$ modelling based on the element of time characterised by $p$ nodal points. Therefore, the vector $\boldsymbol{\beta}_p$ is of order $M \times 1$ with $M = 3p - 2$ and may be estimated through the samples of the input/output signals processed by using the well known ordinary least square (LS) method.

### 3.1. Model parameter estimation

To estimate the parameter vector $\boldsymbol{\beta}_p$, the LS method require writing $M + \nu$ independent equations of (13) type, where $\nu \geqslant 1$ is the number of degrees of freedom for a fit to the model $\mathcal{M}_p$ with $M$ constant parameters. In matrix form, we have

$$\mathbf{q}_p = \mathbf{X}_p\boldsymbol{\beta}_p \tag{14}$$

where the vector $\mathbf{q}_p$ containing the heat fluxes measured is of $(M + \nu) \times 1$ order and is linked to the vector containing the $M$ unknown parameters through the matrix $\mathbf{X}_p$ of order $(M + \nu) \times M$ . The ordinary least square solution to Eq. (14) is given by the following vector [13]:

$$\hat{\boldsymbol{\beta}}_p = \left(\mathbf{X}_p^{\mathrm{T}}\mathbf{X}_p\right)^{-1}\mathbf{X}_p^{\mathrm{T}}\mathbf{q}_p \tag{15}$$

It allows an estimate $\hat{\mathbf{q}}_p$ of the experimental vector $\mathbf{q}_p$ to be derived, that is

$$\hat{\mathbf{q}}_p = \mathbf{X}_p\hat{\boldsymbol{\beta}}_p \tag{16}$$

A quantitative index of the $\hat{\mathbf{q}}_p$ fit to the measured data $\mathbf{q}_p$ may be given by the sum of squares of residuals [13]

$$R_{\mathrm{LS}}(\hat{\boldsymbol{\beta}}) = (\mathbf{q} - \hat{\mathbf{q}})^{\mathrm{T}}(\mathbf{q} - \hat{\mathbf{q}}) = \mathbf{q}^{\mathrm{T}}\left[\mathbf{I} - \mathbf{X}\left(\mathbf{X}^{\mathrm{T}}\mathbf{X}\right)^{-1}\mathbf{X}^{\mathrm{T}}\right]\mathbf{q} \tag{17}$$

More information can be conveyed regarding each parameter $\beta$ by specifying the corresponding confidence interval [14]. The confidence interval on a parameter is an interval constructed from the sample data, within which the true parameter value lies with predetermined probability or degree of confidence. It can be evaluated considering that the quantity $(\hat{\beta}_i - \beta_i)/\hat{\sigma}_{\beta_i}$ has the Student distribution whit $\nu$ degrees of freedom, $\hat{\sigma}^2_{\beta_i}$ being the $i$th diagonal element of $(\mathbf{X}^{\mathrm{T}}\mathbf{X})^{-1}s^2$. The sample variance $s^2$ can be calculated as $R_{\mathrm{LS}}(\hat{\boldsymbol{\beta}})/\nu$. Thus, the $100(1-\alpha)\%$ confidence limits on $\beta_i$ are found by solving the following probability statement:

$$\Pr\left[-t_{1-\alpha/2}(\nu) < \frac{\hat{\beta}_i - \beta_i}{\hat{\sigma}_{\beta_i}} < t_{1-\alpha/2}(\nu)\right] = 1 - \alpha$$

where $t_{1-\alpha/2}(\nu)$ is the inverse of Student's $T$ cumulative distribution function with $\nu$ degrees of freedom and probability $1 - \alpha/2$ in each tail. Rewriting the probability equation to solve for $\hat{\beta}_i - \beta_i$, the $100(1-\alpha)\%$ confidence interval on $\beta_i$ is

$$I_{1-\alpha}(\beta_i) = 2\hat{\sigma}_{\beta_i} \cdot t_{1-\alpha/2}(\nu)$$

The last equations reveal that, for a given model (i.e., given $\hat{\sigma}_{\beta_i}$ value), the reliability of the estimate increases (namely, the corresponding $I_{1-\alpha}$ decreases) when the number of measured data sets (namely, $\nu$) increases. In fact, $t_{1-\alpha/2}(\nu)$ presents high values for low $\nu$ and decreases very quickly up to $\nu \sim 40$ when the $T$ cumulative distribution function assumes quasi-steady values. For $\nu > 40$ the confidence interval decreases slowly as $\nu^{-1/2}$. For assigned degrees of freedom the reliability of the estimate increases if an optimum model for the wall under consideration is found (i.e., minimised $R_{\mathrm{LS}}$ values).

### 3.2. Determining the model dimension

The choice of an appropriate model dimension is most crucial for successful thermal resistance estimation.

In Ref. [9] it was shown that the optimum value $\hat{p}$ of $p$ (usually included between 2 and 6) is a complicated function of the features of the system, of the thermal properties of the system materials and of $\Delta t$. In this case, the system is not known and, consequently, $\hat{p}$ may be estimated solely by the use of measured data applying typical tools of statistics.

To this aim, let be $\boldsymbol{\beta}_{p-1}$ the vector of the parameters appearing in the $\mathcal{M}_{p-1}$ modelling based on the element of time of Fig. 1 characterised by $p-1$ nodal points. In such a circumstance, the parameter vector $\boldsymbol{\beta}_p$ of $\mathcal{M}_p$ may be partitioned as

$$\boldsymbol{\beta}_P^{\mathrm{T}} = \{\boldsymbol{\beta}_{p-1}^{\mathrm{T}}, \boldsymbol{\beta}^*\} \tag{18}$$

Therefore, Eq. (14) is equivalent to

$$\mathbf{q}_p = \mathbf{X}_p\boldsymbol{\beta}_p = \left[\mathbf{X}_{p-1}, \mathbf{X}^*\right]\left\{\begin{array}{c}\boldsymbol{\beta}_{p-1}\\ \boldsymbol{\beta}^*\end{array}\right\} \tag{19}$$

where $\boldsymbol{\beta}^*$ is of $3 \times 1$ order. Now, if we give a known value to $\boldsymbol{\beta}^*$, i.e.,

$$\boldsymbol{\beta}^* = \tilde{\boldsymbol{\beta}}^* \tag{20}$$

then Eq. (19) becomes

$$\mathbf{q}_p - \mathbf{X}^*\tilde{\boldsymbol{\beta}}^* = \mathbf{X}_{p-1}\boldsymbol{\beta}_{p-1} \tag{21}$$

Analogously to Eq. (15), the previous equation allows the parameter vector $\boldsymbol{\beta}_{p-1}$ of $\mathcal{M}_{p-1}$ to be derived as

$$\hat{\boldsymbol{\beta}}_{p-1}(\tilde{\boldsymbol{\beta}}^*) = \left(\mathbf{X}_{p-1}^{\mathrm{T}}\mathbf{X}_{p-1}\right)^{-1}\mathbf{X}_{p-1}^{\mathrm{T}}\left(\mathbf{q}_p - \mathbf{X}^*\tilde{\boldsymbol{\beta}}^*\right) \tag{22}$$

It may be noted that the result of Eq. (22) is strictly linked to the choice expressed by Eq. (20). Dealing with this choice, the sum of squares of residuals is given by

$$R_{\mathrm{LS}}\left[\hat{\boldsymbol{\beta}}_{p-1}(\tilde{\boldsymbol{\beta}}^*)\right] = \left(\mathbf{q}_p - \mathbf{X}^*\tilde{\boldsymbol{\beta}}^*\right)^{\mathrm{T}} \times \left[\mathbf{I} - \mathbf{X}_{p-1}\left(\mathbf{X}_{p-1}^{\mathrm{T}}\mathbf{X}_{p-1}\right)^{-1}\mathbf{X}_{p-1}^{\mathrm{T}}\right]\left(\mathbf{q}_p - \mathbf{X}^*\tilde{\boldsymbol{\beta}}^*\right) \tag{23}$$

At this stage, it is fundamental to verify that the $\mathcal{M}_{p-1}$ modelling be in every practical respect suitable to describe the considered system. By using a mathematical formalism, we should verify the following hypothesis [15]:

$$\mathrm{H}_0: \quad \tilde{\boldsymbol{\beta}}^* = 0 \tag{24}$$

However, from a merely intuitive viewpoint, we can say that the hypothesis $\mathrm{H}_0$ will be rejected if the $R_{\mathrm{LS}}[\hat{\boldsymbol{\beta}}_{p-1}(\tilde{\boldsymbol{\beta}}^*)]$ related to the $\mathcal{M}_{p-1}$ modelling with $\nu$ degrees of freedom is significantly greater than the corresponding $R_{\mathrm{LS}}(\hat{\boldsymbol{\beta}}_p)$ related to the $\mathcal{M}_p$ modelling with $\nu - 3$ degrees of freedom. Formally, $\mathrm{H}_0$ will be rejected if the statistic

$$F = \frac{[R_{\mathrm{LS}}(\hat{\boldsymbol{\beta}}_{p-1}(\tilde{\boldsymbol{\beta}}^* = 0)) - R_{\mathrm{LS}}(\hat{\boldsymbol{\beta}}_p)]/\nu_1}{R_{\mathrm{LS}}(\hat{\boldsymbol{\beta}}_p)/\nu_2} \tag{25}$$

(with $\nu_1 = 3$ and $\nu_2 = \nu$) is greater than critical value $F_{1-\alpha}(\nu_1, \nu_2)$, where $\alpha$ represents the significance level of the test. The more the value of $\alpha$ is low (as an example, $\alpha = 0.05$ or also $\alpha = 0.01$), the more the probability to reject the hypothesis $\mathrm{H}_0$ (when $\mathrm{H}_0$ is true) is low. The values of $F_{1-\alpha}(\nu_1, \nu_2)$ as functions of $\alpha, \nu_1$ and $\nu_2$ are available in a both graphical and tabular form in the specialised literature [16].

Since we have to select the appropriate model increasing the chain structure, the applicability of the above procedure requires that a starting model is fixed preliminarily. Although setting $p = 2$ is the more obvious way to do this, such a choice cannot be always appropriate.

### 3.3. Quality criteria

Once the model dimension has been selected and the vector of the parameters has been estimated, quantitative criteria must be available to establish when, from a statistical point of view, the quality of the obtained estimate has reached a satisfactory level and, therefore, the measurements can be stopped.

Directing attention towards the thermal resistance $R$ and recalling the meaning of confidence interval on a generic parameter, one may assume that $\widehat{R}$ is a reliable estimate of $R$ at the 1% level of significance if the ratio $I_{0.99}(R)/\widehat{R}$ is smaller than a preestablished value (for example, 0.05 or 0.01). Since in any single application a single interval either includes the parameter values or it does not, a number $N$ of such reliable estimates can be found, each of them corresponding to a different number of experimental data sets (namely, different degrees of freedom) and/or different models (namely, different $p$ values).

Setting $w_i = 1/I_{1-\alpha}(R_i)$ as uncertainly of $i$th estimate $\widehat{R}_i$, the weighted average $\overline{R} = \sum_{i=1}^{N} w_i\widehat{R}_i / \sum_{i=1}^{N} w_i$ can be assumed as the final estimate of $R$ provided $N$ is enough great to make the uncertainly of the mean $1/\sum_{i=1}^{N} w_i$ less than $\varepsilon$% of $\overline{R}$ , where $\varepsilon$% depends on the desired estimate accuracy (for example, $\varepsilon = 1\%$).

Unfortunately, such a simple criterion is not always sufficient. In fact, once an erroneous estimate (20% or higher) has been observed after a very short period of measurement analysing the heavy wall. The reason for this erroneous result is due to both the assumed starting model ($p = 2$, typical of very light walls) and a limited period of measurement (8–10 h) during which the input/output signals were characterised by a quasi-steady trend.

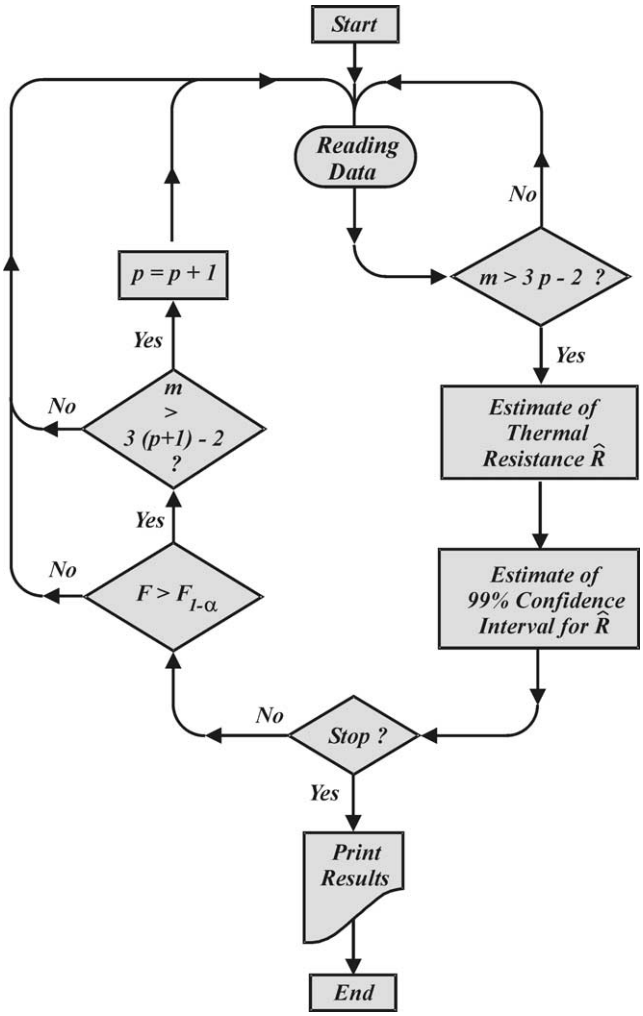


Fig. 2. Flow chart of the proposed procedure.

Summarising, to avoid such erroneous estimates, an appropriate starting model would be adopted with the only exception of very light building elements. To limiting the consequences of this choice on the measurement length, suitable starting $p$ values would be 5 to 15 passing from light to heavy walls.

Fig. 2 shows a flow chart of the whole proposed procedure where the various steps of the calculation as well as their logical sequence and reciprocal interaction are well put into evidence.

## 4. Applications and results

The methodology developed by the authors in the previous sections has been applied to the test data sets given in Ref. [7]. In particular, these data sets refer to three different walls whose thermal properties are shown in Table 1. The first wall is a light, well-insulated one; the second is a massive wall with insulation layers on both sides; the third is a moderately massive homogeneous wall. As remarked in [7] these walls are not intended to cover the most real building elements, but they represent the critical elements for a dynamic analysis method.

The samples of the inner and outer surface temperatures (independent variables) as well as the ones of the inner surface heat flux (dependent variable) are given in the form of a Fourier series whose first 37 harmonics have a period $T$ variable in the range $T \in [3, 8736\ \text{h}]$. Therefore, experimental data simulated per an entire year are available.

In order to simulate a number of measurement runs, 24 data sets containing temperatures and heat flux have been generated for each wall. Data sets start every 360 h and present a 15-days duration. For each of the above data sets, Fig. 3 shows the average of the indoor/outdoor temperature differences. It has a great influence on both the measurement length and the results accuracy, and always falls between 0.14 and 21.6 K.

The dynamic method here proposed has been applied to each of the three walls of Table 1 assuming as input and output signals the 24 data sets summarised above. For each wall we have obtained 24 estimates which present the percent deviations, namely, $(\overline{R} - R)/R \times 100$, depicted in Fig. 4. As it can be seen, the lowest deviations refer to the light wall (generally $\pm 0.10\%$ or less), while the highest ones refer to the heavy wall (the second of Table 1) and vary from $\pm 0.1\%$ to about $\pm 3.5\%$. The highest values refer generally to the measurement periods characterised by the lowest indoor/outdoor temperature differences.

Both the wall characteristics and temperature differences affect the measurement length. As shown in Fig. 5, suitable

Table 1
Thermal properties of the reference walls (i.e., 1, 2, 3) given in Ref. [6]

| $N$ | *Material* | $s$ (m) | $k$ (W·m$^{-1}$·K$^{-1}$) | $\rho$ (kg·m$^{-3}$) | $c$ (J·kg$^{-1}$·K$^{-1}$) | $R$ (m$^2$·K·W$^{-1}$) |
|---|---|---|---|---|---|---|
| 1 | Facing | 0.01 | 0.100 | 600 | 1000 | 11.6286 |
| | Insulation | 0.40 | 0.035 | 30 | 1000 | |
| | Facing | 0.01 | 0.100 | 600 | 1000 | |
| 2 | Facing | 0.01 | 0.100 | 600 | 1000 | 6.3429 |
| | Insulation | 0.05 | 0.035 | 30 | 1000 | |
| | Masonry | 0.30 | 0.700 | 1800 | 1000 | |
| | Insulation | 0.15 | 0.035 | 30 | 1000 | |
| | Facing | 0.01 | 0.100 | 600 | 1000 | |
| 3 | Masonry | 0.40 | 0.200 | 800 | 1000 | 2.0000 |

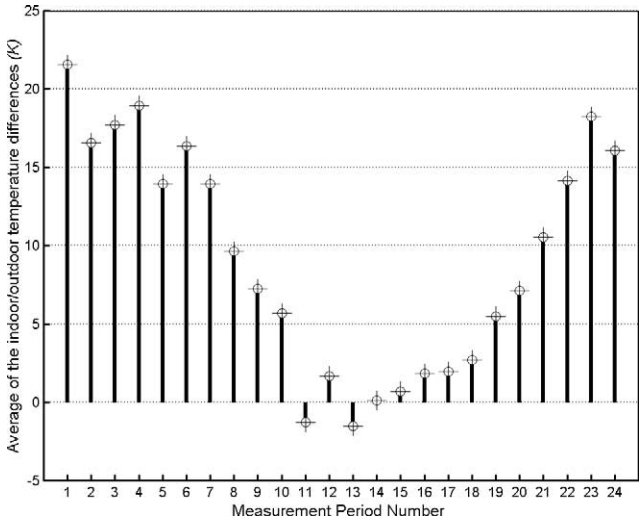


Fig. 3. Average of the indoor/outdoor temperature differences for 24 simulated measurement periods [7], each starting every 360 h and having a 15-days length.

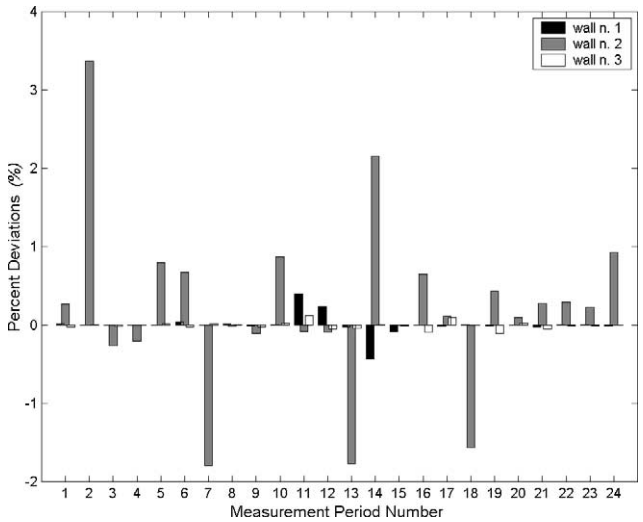


Fig. 4. Percent deviations between the true thermal resistances (of the walls of Table 1) and ones estimated through the present dynamic method assuming as input/output signals the 24 data sets of Fig. 3.

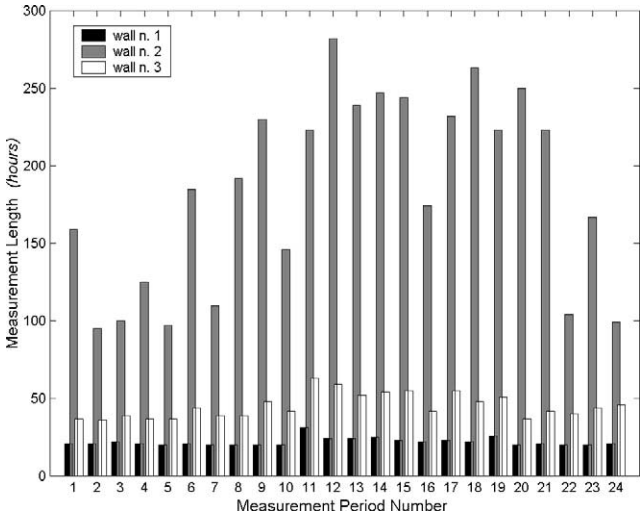


Fig. 5. Measurement periods required to obtain the percent deviations of Fig. 4.

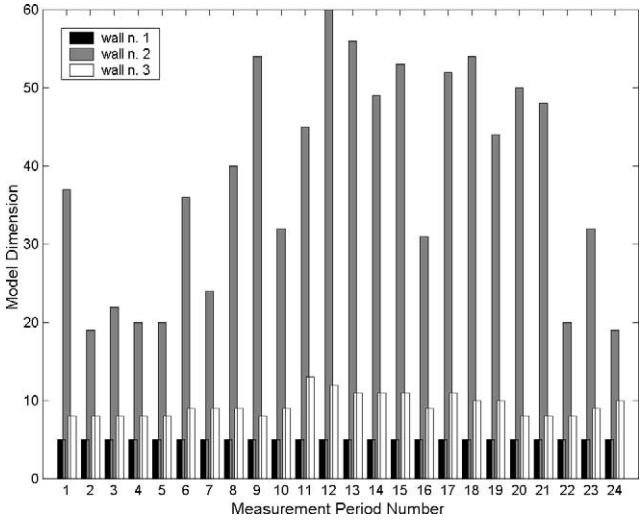


Fig. 6. Model dimension reached during the measurement periods of Fig. 5.

estimates are generally reached in short measurement periods (20–30 h) for the light wall independently of the climatic period. For the medium wall (third of Table 1), 50 h are generally sufficient to reach a suitable estimate, but they can also increase up to 90 h for typically summer periods of measurement. Instead, sufficiently long measurement periods characterise the heavy wall. They, in fact, vary from 80–100 h (first 20 and last 6 weeks of the year) to 240–300 h (summer season).

Analogous considerations can be made for the model dimension illustrated in Fig. 6. It should be noted that the model dimension rarely exceeds $p = 5$ and $p = 10$ for the light and medium walls, respectively, independently of the indoor/outdoor temperature differences. For the heavy wall, instead, very high values of $p$ are generally observed in summer measurement periods.

However, it may be noted that the dimensions of the models that have allowed the results plotted in Figs. 3–6 to be obtained are much higher (generally 2–4 times) than the conventional dimensions found in Refs. [8,10]. The reason is that the $p$ value is affected not only by the inherent features of the analysed wall, but also and above all by the ones of the input/output signals (concerning this, we recall that the $p$ value is derived exactly from these signals, as discussed in Section 3.2).

For the sake of brevity, the time history of the estimated $\widehat{R}$ has been performed for only the heavy wall, assuming as input signals the data set 1 (highest temperature difference) and the data set 14 (lowest temperature difference) of Fig. 3. Starting from $p = 15$, as the measured data become available, the model dimension increases if the corresponding test requires it (Section 3.2). The results are summarised in

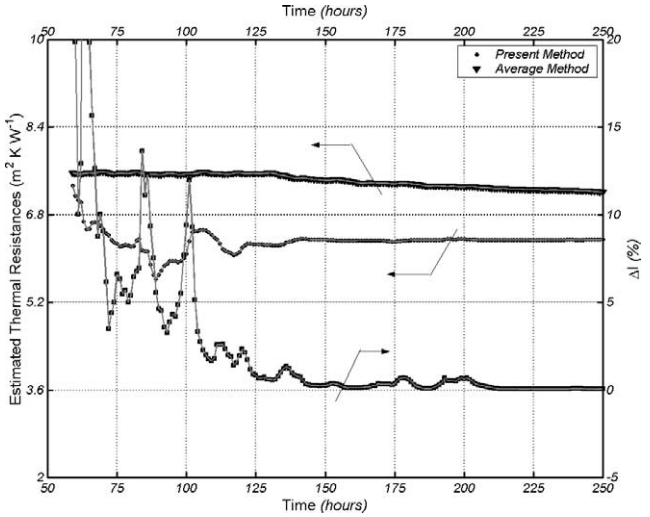


Fig. 7. History of the thermal resistance of wall 2 estimated through both the present method and the average one during a 250 h-long measurement (period 1 of Fig. 3—winter period).

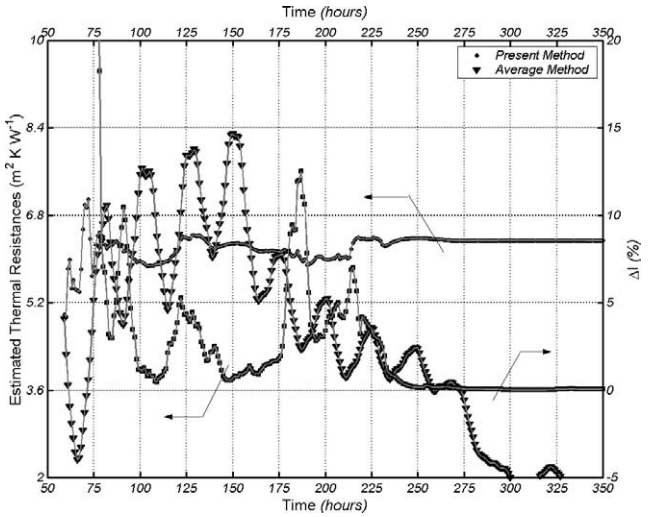


Fig. 8. History of the thermal resistance of wall 2 estimated through both the present method and the average one after a 350 h-long measurement (period 14 of Fig. 3—summer period).

Figs. 7 and 8, respectively. In particular, these figures show the ratio $\Delta I = I_{0.99}(R)/\widehat{R} \times 100$. Comparing the results obtained for the winter and summer periods we can observe the influence of the indoor/outdoor temperature difference on both the scatter of the results and the measurement length to achieve a stable estimate. It can be remarked firstly that, for the early hours, both the width of the confidence interval and the corresponding thermal resistance estimate are highly variable. This is an expected result because of the model unsuitableness and low $\nu$ values (see Section 3.1). The length of such an instability period generally increases, for a given wall, passing from the winter period (120 h) to the summer one (225 h, in the examined cases). For a given data set, the instability period length increases passing from the light wall to the heavy one.

It should be noted that Figs. 7 and 8 give the same results obtained through the following equation:

$$\widehat{R} = \frac{\sum_{j=1}(T_{\mathrm{is},j} - T_{\mathrm{os},j})}{\sum_{j=1} q_j} \tag{26}$$

which represents the starting step of the average method. In particular, it assumes that the ratio of the mean of the temperature differences on the mean of the surface fluxes goes asymptotically towards the value of the searched thermal resistance. A comparison with the average method shows that, against an acceptable complication of calculation, the methodology here proposed is able: (1) to reduce considerably the stop periods of the test facilities (see Fig. 7), and (2) to reach the results also in the heaviest seasonal periods (i.e., summer), which instead make the average method completely ineffective (see Fig. 8). The above conclusions valid only for a single wall can readily be extended to the other walls of Table 1. In fact, once the average method is applied to the previous 24 data sets for each wall of Table 1, the following results can be pointed out. The measurement length assumes the same order of magnitude of the one which has been obtained by means of the dynamic method here proposed, if the average of the indoor/outdoor temperature difference is greater than 10 K and if a percent deviation of about $\pm 5\%$ up to $\pm 10\%$ (or a bit more) can be accepted. As the average of the indoor/outdoor temperature differences decreases, the measurement length quickly increases if the percent deviations would be retained within the previous limitations. When the average of the indoor/outdoor temperature differences is lower than 5 K (periods 11 up to 19 of Fig. 3), the average method cannot be used even for light walls.

## 5. Conclusions

In this paper a method for the dynamic analysis of in-situ data was developed in order to determine the thermal resistance of walls.

Initially the method was applied to simulated data provided by the proposal of European standard "prEN 12494, 1996," which were referring to three different typologies of wall. The first is a light, well-insulated one; the second is a massive wall with insulation layers on both sides; the third is a moderately massive homogeneous wall.

To simulate a number of measurement runs, 24 data sets containing surface temperatures and heat flux have been generated for each wall. Data sets start every 360 h and present a 15-days length. They present an average of the indoor/outdoor temperature differences which oscillates between 0.14 and 21.6 K.

The following conclusions can be pointed out from the obtained results:

– the dynamic method here proposed allows reliable values of the wall thermal resistance to be obtained for

every set of 24 simulated data. The percent deviations between the true and calculated thermal resistances are very low for the light wall (generally ±0.10% or less). The highest errors are instead obtained for the heavy wall (±0.1% to about ±3.5%). Higher values refer generally to the measurement periods characterised by lower indoor/outdoor temperature differences;

– reliable values of the thermal resistance generally require short measurement periods (20–30 h) for the light wall independently of the climatic period. For the medium wall, instead, 50 h are generally required to reach a reliable value. However, 90 h can also be required for typically summer periods of measurement. Finally, quite long measurement periods characterise the heavy wall: from 80–100 h (first 20 and last 6 weeks of the year) to 240–300 h (summer season);
– a comparison with the well-known average method puts into evidence that the measurement length assumes the same order of magnitude of the one obtained through the dynamic method here proposed if the average of the indoor/outdoor temperature difference is greater than 10 K and if percent deviations of about ±5% up to ±10% can be accepted. However, when the average of the indoor/outdoor temperature differences is lower than 5 K, the average method cannot be used.

Further developments of the proposed method will be concerning its validation with actually measured data (not simulated). To this purpose, a test facility is already at a advanced level of preparation.

## References

[1] ISO standard 8301–1991, Thermal insulation—determination of steady-state thermal resistance and related properties—heat flow meter apparatus.

[2] ISO standard 8302-1991, Thermal insulation—determination of steady-state thermal resistance and related properties—guarded hot plate apparatus.

[3] ISO standard 8990-1994, Thermal insulation—determination of steady-state thermal resistance and related properties—calibrated and guarded hot box.

[4] L. Ljung, System Identification—Theory for the User, Prentice Hall, New Jersey, 1999.

[5] ISO standard 9869-1994, Thermal insulation—building elements—in situ measurement of thermal resistance and thermal transmittance.

[6] C. Roulet, J. Gass, I. Marcus, In situ $U$-value measurement: reliable results in shorter time by dynamic interpretation of the measured data, ASHRAE Trans. 108 (1987) 1371–1379.

[7] prEN standard 12494-1996, Building components and elements—in-situ measurement of surface-to-surface thermal resistance.

[8] F. Marcotullio, A. Ponticiello, Determination of transfer functions in multidimensional heat conduction by means of a finite element technique, in: R.W. Lewis, et al. (Eds.), Proceedings of Numerical Methods in Thermal Problems, Part I, vol. VIII, Pineridge Press, Swansea, UK, 1993, pp. 226–236.

[9] L. Laurenti, F. Marcotullio, P. Zazzini, A proposal for the calculation of panel heating and cooling system based on transfer function method, ASHRAE Trans. 108 (1) (2002) 183–201.

[10] L. Laurenti, F. Marcotullio, A. Ponticiello, Multi-dimensional transient conduction analysis by generalized transfer functions tables, J. Heat Transfer 119 (1997) 238–241.

[11] O.C. Zienkiewicz, The Finite Element Method, McGraw-Hill, London, 1977.

[12] S.S. Rao, The Finite Element Method in Engineering, Pergamon Press, New York, 1989.

[13] J.V. Beck, K.J. Arnold, Parameter Estimation in Engineering and Science, Wiley, New York, 1977.

[14] Matlab Statistics Toolbox User's Guide, Version 2.1, MathWorks, Natik, MA, 1997.

[15] J.L. Jaech, Statistical Analysis of Measurement Errors, Wiley, New York, 1985.

[16] P.R. Bevington, Data Reduction and Error Analysis for the Physical Sciences, McGraw-Hill, New York, 1969.